At-sea intercomparison of two newly designed underway pCO_2 systems — encouraging results

Arne Körtzinger [a,*], Helmuth Thomas [b], Bernd Schneider [b], Nicole Gronau [b], Ludger Mintrop [a], Jan C. Duinker [a]

[a] *Institute for Marine Sciences at Kiel University, Department of Marine Chemistry, Düsternbrooker Weg 20, D-24105 Kiel, Germany*
[b] *Baltic Research Institute at Rostock University (IOW), Chemistry Section, Seestraße 15, D-18119 Warnemünde, Germany*

Abstract

Two newly designed underway systems for the measurement of CO_2 partial pressure (pCO_2) in seawater and the atmosphere are described. Results of an intercomparison experiment carried out in the North Sea are presented. A remarkable agreement between the two simultaneously measured pCO_2 data sets was observed even though the spatial variability in surface pCO_2 was high. The average difference of all 1-min averages of the seawater pCO_2 was as low as 0.15 μatm with a standard deviation of 1.2 μatm indicating that no systematic difference is present. A closer examination of the profiles shows that differences tend to be highest during maxima of the pCO_2 gradient (up to 14 μatm/min). The time constants of both systems were estimated from laboratory experiments to 45 s, respectively, 75 s thus quantitatively underlining their capability of a fast response to pCO_2 changes.

1. Introduction

Due to the burning of fossil fuel and the human impact on land biota the atmospheric concentration of CO_2 is steadily increasing (e.g. Keeling et al., 1995). As the major greenhouse gas except water vapor CO_2 interacts strongly with the radiative balance of the earth and its increasing concentration potentially influences the global climate. However, only about 45% of the total anthropogenic emissions of CO_2 remains airborne (Houghton et al., 1990). The ocean has long since been recognized as an important sink for a significant portion of the miss-

ing anthropogenic CO_2. Being the largest rapidly exchanging reservoir of carbon it will in a future steady state absorb in the order of 85% of all manmade CO_2. However, with a mean ventilation time of the world ocean of 500–1000 years as the main kinetic barrier the ocean cannot keep pace with the atmospheric perturbation. Therefore the understanding of the oceans' role in the global carbon cycle has become — as we feel — one of the most thrilling challenges in marine sciences.

The concepts in tracing and quantifying the anthropogenic carbon dioxide in the ocean are manifold and most of them are based on assumptions and parametrizations that are still not unequivocally accepted. One concept that receives particular attention among research groups not only since the intriguing

* Corresponding author. Tel.: + 49-431-5974023; fax: + 49-431-565876; e-mail: akoertzinger@ifm.uni-kiel.d400.de.

findings of Tans et al. (1990) is the ΔpCO_2 concept: the net flux of CO_2 across the air–sea interface is proportional to the difference of the partial pressures of CO_2 (ΔpCO_2) in the atmosphere and the surface water. If we were able to cover the world ocean with a grid of representative mean ΔpCO_2 values and further could assign appropriate exchange coefficients to them the global net flux of CO_2 across the air–sea interface could be calculated (Watson et al., 1995). However, if in the light of the considerable spatiotemporal variability of ΔpCO_2 this concept shall be successful a broad data base has to be generated. Only if a combined effort of research groups around the world leads to ΔpCO_2 profiles across all parts of the world ocean and at different seasons the estimate of the anthropogenic CO_2 flux into the ocean can possibly be pinned down more precisely.

In this context the question of comparability of pCO_2 data from different laboratories and different analytical systems plays a vital role for the success of the ΔpCO_2 concept. The mean global air–sea ΔpCO_2 necessary to accommodate a global oceanic sink of 2.0 Gt C yr^{-1} is in the order of 7 μatm (Wallace, 1995). This is a rather small signal compared to an analytical precision in the order of 1 μatm and an accuracy of probably not better than a few μatm. To assess the current state an international intercomparison exercise, marvellously organized by A. Dickson and co-workers (Scripps Institution of Oceanography, Marine Physical Laboratory, La Jolla/California, USA, June 6–10, 1994), was carried out as a first step. In this paper we report data from a 21-h intercomparison experiment which was carried out at sea with two newly designed underway pCO_2 systems. The results clearly show that at least with systems of similar design highly comparable measurements are possible.

2. Theoretical background

The partial pressure of an ideally behaving component i is defined as the product of its mole fraction x_i and the total pressure of the gas phase. As the partial pressure is defined for the gas phase only the term "seawater partial pressure" of a volatile component means the partial pressure of this component in a gas phase which is in equilibrium with seawater with respect to this component. To take into account the non-ideal character of a gas like CO_2 the fugacity should be used rather than the partial pressure (DOE, 1994). It can be calculated from an equation given by Weiss (1974). Since the difference is rather small most data presented in the literature are still given as pCO_2 values instead of fCO_2 values.

The net flux F of CO_2 across the air–sea interface can be calculated from the partial pressure difference between seawater and atmosphere:

$$F = k \cdot K^0 (\Delta pCO_2)$$

where k is the transfer velocity, K^0 is the solubility coefficient of CO_2 in seawater and ΔpCO_2 is the difference of pCO_2 in the corresponding bulk layers (i.e., surface mixed layer and air). The partial pressure difference ΔpCO_2 is the thermodynamic driving force of the net gas flux. The transfer velocity k mainly depends on wind speed and seawater temperature (Liss, 1983; Liss and Merlivat, 1986; Wanninkhof, 1992) while K^0 depends on temperature and salinity (Weiss, 1974).

3. Materials and methods

3.1. The systems

The principle of pCO_2 measurement is based on the equilibration of a carrier gas phase with a seawater sample and subsequent determination of the CO_2 volume mixing ratio in the carrier gas. As the pCO_2 in seawater strongly varies with temperature a correction is necessary to compensate for the difference between equilibration temperature and the in-situ seawater temperature. Different equations have been proposed for the temperature dependence of CO_2 partial pressure/fugacity in seawater (Gordon and Jones, 1973; Weiss et al., 1982; Copin-Montegut, 1988, 1989; Goyet et al., 1993; Takahashi et al., 1993).

A great variety of pCO_2 systems and equilibrators has been described in the literature. Essentially three different design principles can be distinguished, i.e., (1) the "shower type" equilibrator (e.g., Keeling et al., 1965; Kelley, 1970; Weiss, 1981; Inoue et

al., 1987; Robertson et al., 1993; Goyet and Peltzer, 1994), (2) the "bubble type" equilibrator (e.g., Takahashi, 1961; Goyet et al., 1991; Schneider et al., 1992; Kimoto and Harashima, 1993; Ohtaki et al., 1993), and (3) the "laminary flow type" equilibrator

(Poisson et al., 1993). A design described by Copin-Montegut (1985) combines aspects of the shower and bubble type.

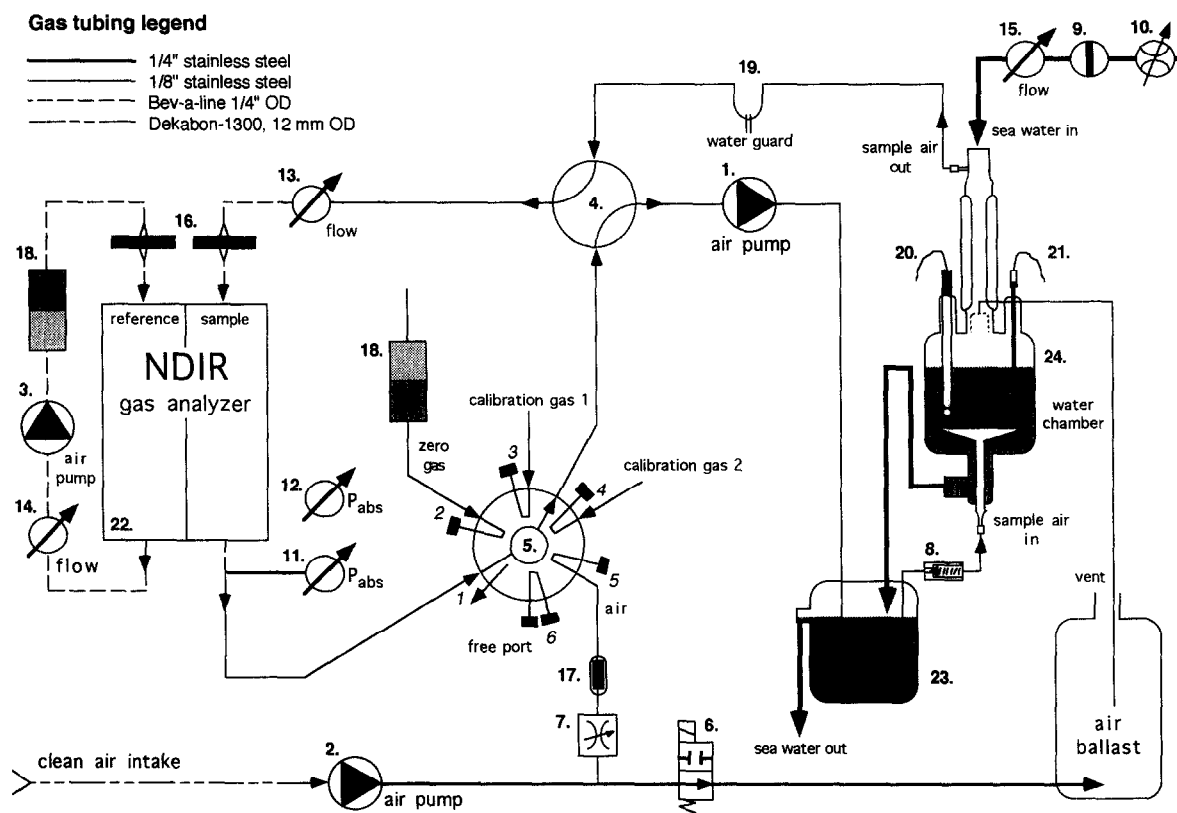Two underway pCO_2 systems, developed independently at the Institute for Marine Sciences, Kiel

Fig. 1. Schematic diagram of the Kiel underway system (IFM) for the determination of pCO_2 in seawater and air. 1. Air pump, max. flow = 9.0 l/min, Δp max. = 780 mbar, Erich Fürgut Miniaturgaspumpen, Aitrach, Germany. 2. Air Cadet[*] pump, max. flow = 22 l/min, Δp max. = 600 mbar, Cole-Parmer International, Niles, IL, USA. 3. Air pump, max. flow = 1.6 l/min, Δp max. = 100 mbar, Erich Fürgut Miniaturgaspumpen, Aitrach, Germany. 4. 2-position valve, electric actuator, Valco Instruments Co. Inc., Houston, TX, USA. 5. Multiposition valve (6 positions, 13 ports, flow-through flowpath), electric actuator, Valco Instruments Co. Inc., Houston, TX, USA. 6. 2-way PTFE solenoid valve, normally open, Neptune Research Inc., Maplewood, NJ, USA. 7. Needle valve with calibrated micrometer head, NUPRO Company, Willoughby, OH, USA. 8. Check valve, opening pressure 20 mbar, NUPRO Company, Willoughby, OH, USA. 9. Ball valve, manually actuated. 10. Flow controller (0.2–2.0 l/min), Cole-Parmer International, Niles, IL, USA. 11, 12. Pressure transducer (600–1100 mbar, accuracy 0.05% full scale), Setra Systems Inc., Acton, MA, USA. 13. Gas flowmeter with needle valve (10–100 l/h), Kobold Meßring GmbH, Hofheim, Germany. 14. Gas flowmeter with needle valve (33–430 ml/min), Kobold Meßring GmbH, Hofheim, Germany. 15. Liquid flowmeter (0.25–2.5 l/min), Kobold Meßring GmbH, Hofheim, Germany. 16. PTFE membrane filter (1 μm), Gelman Sciences, Ann Arbor, MI, USA. 17. Particle filter (2 μm), NUPRO Company, Willoughby, OH, USA. 18. Gas purification tube with CO_2 scrubber (Ascarite II[*], Aldrich-Chemie GmbH, Steinheim, Germany) and chemical desiccant ($Mg(ClO_4)_2$, dto). 19. Water guard (platinum electrodes in U-shaped glass tube). 20. pH glass electrode (ROSS series, ORION Research Inc., Boston, MA, USA) with pH/mV meter 530, Wissenschaftlich-Technische Werkstätten GmbH, Weilheim, Germany. 21. Pt-100 temperature probe (4-wire technique) with temperature monitor, Burster Präzisionsmeßtechnik GmbH and Co. KG, Gernsbach, Germany. 22. NDIR CO_2/H_2O gas analyzer, model LI-6262, LI-COR Inc., Lincoln, NE, USA. 23. Reservoir. 24. Equilibrator (made of DURAN[*] glass, consisting of water chamber and column with evacuated jacket).

(IFM) and at the Baltic Sea Research Institute, Warnemünde (IOW) were used in the present inter-comparison experiment. Both systems are of the "bubble type" and similar in principle though different in detail. Therefore common aspects will be discussed first. This is followed by two chapters with a more detailed description of the individual design of both systems.

A continuous flow of seawater passes through an open system equilibration cell, which is vented to the atmosphere. This allows the equilibrium process to take place at ambient pressure at any time. A fixed volume of air is re-circulated continuously through the system so as to be in almost continuous equilibrium with the constantly renewed seawater phase. In a "bubble type" equilibrator this airflow is bubbled through the water phase. After passage through the equilibration cell the air stream is pumped to a non-dispersive infrared gas analyzer, where the mole fraction of CO_2 is measured relative to a dry and CO_2-free reference gas (absolute mode). Both systems feature a LI-COR® LI-6262 CO_2/H_2O gas analyzer, which is a dual-channel instrument that simultaneously measures the CO_2 and H_2O mole fractions. The gas stream needs no drying prior to infrared gas detection as the biasing effect of water vapor on the measurement of CO_2 is eliminated based on the H_2O measurement. The appropriate internal algorithms not only correct for dilution of the sample gas by the "additional" (compared to calibration gases) component water but also for gas phase interactions of CO_2 with water vapor which cause a broadening of the absorption band of CO_2 (McDermitt et al., 1993). The various advantages of this particular NDIR system and its perfect seagoing performance have been described in more detail by Goyet and Peltzer (1994). Both gas circuits (components and fittings) were checked for leakages with elevated CO_2 levels in the surrounding air.

3.1.1. The Kiel underway pCO_2 system (IFM)

The schematic drawing in Fig. 1 depicts the general design of the Kiel underway pCO_2 system (hereafter IFM system). All numbers in the description below refer to numbers appearing in Fig. 1.

The equilibrator (24) combines two equilibration concepts which are realized in two subsequent stages. One stage operates as a "bubble type" equilibrator

in which a water chamber is filled with appr. 1000 ml of constantly renewed water. The air enters from below through a coarse glass frit and is bubbled through the water. The second stage acts as a "laminary flow" equilibrator. A 45-cm glass column is centered on top of the water chamber. The seawater enters from the top and forms a laminary flow on the inner walls of the column, while the air coming from the water chamber below passes through the column before it leaves the equilibrator at the head of the column. The counter-current flow direction of seawater and air as well as the large surface area facilitate the establishment of equilibrium. An evacuated jacket minimizes temperature changes of the water flow during passage through the column. Typically the temperatures differ by a few tens of a degree and differences rarely exceed 1°C. The flow rate of seawater is set to 1.5–2.0 l/min. A PC-interfaced flow controller (10) adjusts the flow rate to the pre-set value and compensates for pressure changes which frequently occur when the ship's own seawater pumping systems are used.

The air circuit (total volume approx. 400 ml) is maintained with air pump 1 at a flow rate of 1.0–1.2 l/min. After leaving the equilibrator the air is pumped through water guard 19, valve 4, a flowmeter/needle valve combination (13) and a 1-μm PTFE membrane filter (16) to the NDIR gas analyzer (22). Its CO_2 and H_2O mole fractions are monitored continuously, and the air stream is re-circulated via multiposition valve 5, valve 4 and the air pump (1) to a reservoir (23) which is flushed with waste water from the equilibrator. The gas tubing is coiled within the reservoir to adjust the air stream to the seawater temperature before re-entering the equilibrator. A check valve (8) avoids invasion of water through the frit into the gas lines in case of pump failure.

The reference gas circuit is a closed loop system which consists of a flowmeter/needle valve (14), a miniature air pump (3), a gas purification tube (18) and a 1-μm PTFE membrane filter (16). This feature provides a constant supply of dry and CO_2-free air as a zero reference gas and thus strongly reduces gas requirements to just one set of calibration gases.

For the measurement of ambient atmospheric pCO_2 an Air Cadet® diaphragm pump (2) continuously draws uncontaminated air from the compass platform of the research vessel through a Dekabon®-

type flexible tubing (Furon Dekoron Division, Aurora, OH, USA, 12 mm OD) to the pCO_2 system. When atmospheric pCO_2 is not being measured this air is used to flush the air ballast bottle which provides a clean air buffer to the equilibrator vent. If any volume change occurs in the re-circulated air only clean outside air can invade the system through the vent line. For air measurements valve 6 is closed and the air enters the system via needle valve 7 and a 2-μm pre-filter (17).

Three different types of measurements (calibration, measurement of atmospheric or seawater equilibrated air) are controlled with valves 4 and 5. Fig. 2 is a schematic drawing of the valve concept with the two different general states described below. Valve 4 separates the equilibrator circuit from the measuring circuit. Thus during air measurement or calibration of the system pump 1 keeps the short-circuited equilibration circuit in progress (Fig. 2, right), while the separated measuring circuit is flushed with ambient air respectively calibration gases. Valve 5 selects the gas to be measured.

For measurements of pH and seawater temperature the equilibrator is equipped with a pH glass electrode (20) and a platinum resistance thermometer (21). Two high-accuracy pressure transducers (11, 12) are used to monitor barometric pressure as well as pressure in the NDIR cell.

For automation of the system a special software has been developed. It carries out two different functions: (1) all data generated by the system (raw mV readings, xCO_2, xH_2O, T_{NDIR}, p_{NDIR}, p_{atm}, T_{eq}, pH_{eq}) or provided by the data distribution system of the vessel (GPS latitude and longitude, $T_{in-situ}$, salinity) are interrogated, averaged and logged at user-chooseable intervals. A typical routine comprises an interrogation interval of 6 s and an averaging interval of 1 min; (2) the fully accessible duty cycle is carried out by remote control of the three valves. The duration and interval of measurement states (calibration, measurement of seawater equilibrated or atmospheric air) can be chosen from a set-up menu. A typical routine consists of initial calibration, then 57 min measurement of pCO_2 (seawater) and 3 min measurement of pCO_2 (air) alternating, with re-calibration after 4–6 cycles (i.e., approx. 4–6 h). A delay interval can be defined to avoid logging of data during a time interval after
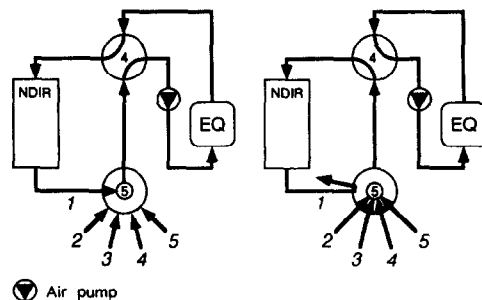

Fig. 2. Valve concept for gas control in the IFM underway pCO_2 system. The interaction of valves 4 and 5 is shown schematically for the measurement of seawater equilibrated air (left) and ambient air resp. calibration gases (right).

valve switching. An interval of 60 s has been shown to be sufficient to allow the reading to re-stabilize after a change of the measured gas.

For calibration of the NDIR instrument a set of three calibration gases is used (CO_2-free air, low and high CO_2 standard gas). All air mixtures are based on the "natural" air concept and contain nitrogen, oxygen and argon in the natural proportions (i.e., 780 pptv N_2, 210 pptv O_2, 9.3 pptv Ar). The CO_2-free air is purified with a CO_2 scrubber (Ascarite II*) and a desiccant (magnesium perchlorate). The LI-COR* instrument comes with an individual calibration polynomial. User calibration consists of setting the "zero" and "span" of the system (low standard gas). Rather than being done manually the "zero" and "span" set is performed automatically by the software during each calibration procedure. The high standard gas is run regularly as a calibration check.

The whole system (except the PC) is contained in a plexiglass/polyethylene chassis that fits almost fully assembled into an aluminium case for easy shipping.

3.1.2. The Warnemünde underway pCO_2 system (IOW)

Fig. 3 shows a schematic drawing of the general design of the Warnemünde underway pCO_2 system (hereafter IOW system). All numbers in the description below refer to numbers appearing in Fig. 3.

3.1.2.1. Water supply. The continuous flow of seawater through the equilibrator is generated by a

submerged pump (2), which is mounted in the moon poole of the vessel. Hence, the seawater is pumped all the way to the equilibrator at overpressure hereby avoiding any outgassing. From the total water flow of 60–100 l/min the sample flow is teed off just in front of the equilibrator and finally adjusted to a flow rate of approx. 1 l/min by means of valve 14. The high flow rate in the main by-pass and additional heat insulation of the tubing keeps the water in the equilibrator close to in situ temperature.

The seawater volume in the equilibrator is given by the height of the water outlet and corresponds to a volume of about 200 ml. In order to increase the efficiency of the water exchange, a pipe connects the water outlet with the water close to the bottom of the equilibrator. At a flow rate of 1 l/min a time constant of 12 s results for the water renewal in the equilibrator. The water from the equilibrator flows through a heat insulated bath which serves as a temperature buffer between the equilibrator and ambient air. The water temperature in the equilibrator is recorded continuously with a precision of 0.05°C. Additionally, pH is measured and used to examine qualitatively consistency with the pCO_2 measurements.

3.1.2.2. Equilibration. A membrane pump (15a) is used to circulate a volume of about 100 ml of air at a flow rate of 200 ml/min through the water column in the equilibrator and the NDIR detection system. Like in the IFM system air is pre-tempered to the seawater temperature before entering the equilibrator. The air is led through a heat exchange coil submerged in the temperature buffer bath. Bubbles in
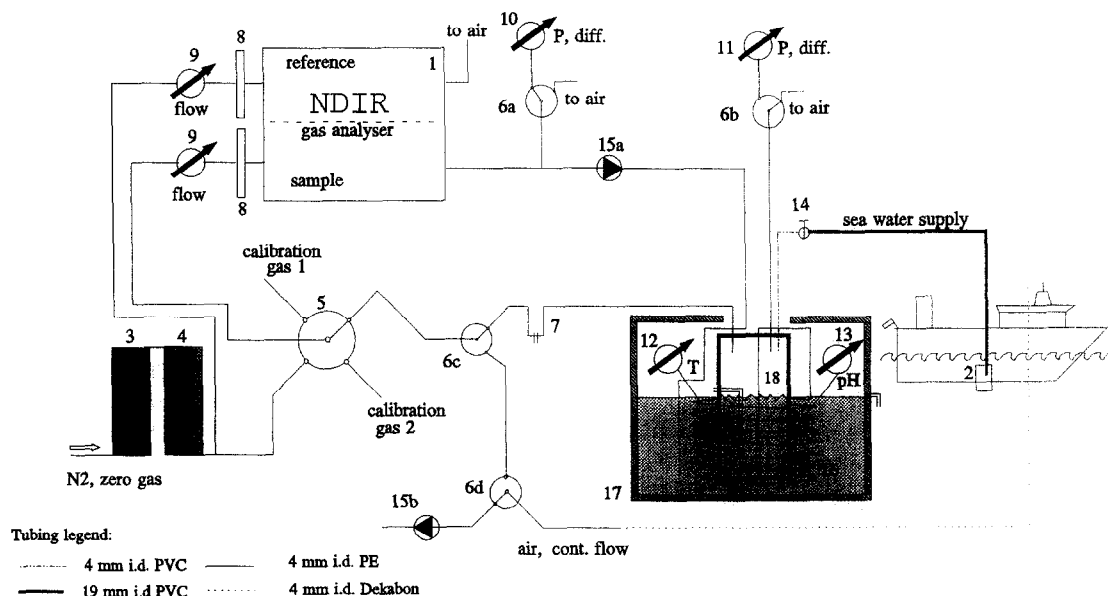

Fig. 3. Schematic diagram of the Warnemünde underway system (IOW) for the determination of pCO_2 in seawater and air. 1. NDIR CO_2/H_2O gas analyzer, model LI-6262, LI-COR Inc., Lincoln, NE, USA. 2. Immersion pump, max. flow = 100 l/min, Flygt GmbH.3. Gas purification tube with CO_2 scrubber (soda lime pellets, Merck, Darmstadt, Germany). 4. Gas purification tube with chemical desiccant (Anhydrone®, J.T. Baker Inc, Phillipsburg, NJ, USA). 5. 5-way ball valve, manually actuated, Whitey Co., Highland Heights, OH, USA. 6a–d. 2-way ball valve, manually actuated, Whitey Co., Highland Heights, OH, USA. 7. Water guard (platinum electrodes in U-shaped glass tube). 8. PTFE membrane filter (1 μm), Gelman Sciences, Ann Arbor, MI, USA. 9. Gas flowmeter with needle valve (0–1 l/min), Dwyer Instruments Inc., Michigan City, USA. 10. Differential pressure transducer (0–50 mbar), model P592-1D-A1A, accuracy 1% full scale, Kavlico Corp., USA. 11. Differential pressure manometer (0–5 mbar), Dwyer Instruments Inc., Michigan City, USA. 12. Pt-100 temperature probe (4-wire technique) with temperature monitor, Burster Präzisionsmeßtechnik GmbH and Co. KG, Gernsbach, Germany. 13. pH glass electrode (model E 56, Wissenschaftlich-Technische Werkstätten GmbH, Weilheim, Germany) with pH/mV meter (model 647, Knick Elektronische Meßgeräte GmbH and Co., Berlin, Germany). 14. Valve, manually actuated. 16. Stainless steel heat exchange coil. 17. Heat insulated bath (Plexiglass®, Styropor®). 18. Equilibrator, glass.

the equilibrator are generated by pressing the air through the capillary tip of a PTFE tube. The air leaving the equilibrator passes a conductivity cell (7) by which the pump is switched off in case of a seawater breakthrough. Via valves 6c and 5, a flow meter (9), and a 1 μm PTFE membrane filter (8) the air enters the IR detector cell. The pressure difference between the exit of the IR cell and ambient air is measured (10) and used together with the barometric pressure from the ship's sensor. The air is re-circulated via pump 15a. Like in the IFM system the equilibrator is open to atmospheric pressure to avoid any over- or underpressure in the headspace. To check this, the pressure difference between the head space and the atmosphere is sporadically measured (11).

For the measurement of atmospheric pCO_2 valves 6c and 6d are switched. Pump 15b continuously pumps clean air from the compass platform out to the system. Calibration is carried like described for the IFM system with a gas flow rate of about 200 ml/min.

3.2. The experiment

The intercomparison experiment was carried out on board R/V Valdivia during cruise no. 148-2 in September, 1994. The 21-h intercomparison experiment was performed on transect A–B in the eastern North Sea (Fig. 4). The R/V Valdivia departed from Kiel on September 11, 1994, and arrived back to Kiel on September 14, 1994, after sailing around Denmark. When designing the experiment care was taken to operate the systems under conditions as comparable as possible. First of all both system were run simultaneously on the water supply system as described in Section 3.1.2.1 for the IOW system. The systems were operated side by side and the water flows required by each of them were teed off right at the systems. In-situ temperature and salinity of the seawater were monitored continuously with a temperature/salinity (conductivity) probe mounted close to the seawater intake. Corrections for temperature changes were performed based on these in-situ temperature readings and the equilibrator temperatures measured and logged by each of the systems. Barometric pressure was taken from the ship's meteorological pressure sensor. Ambient air was drawn from
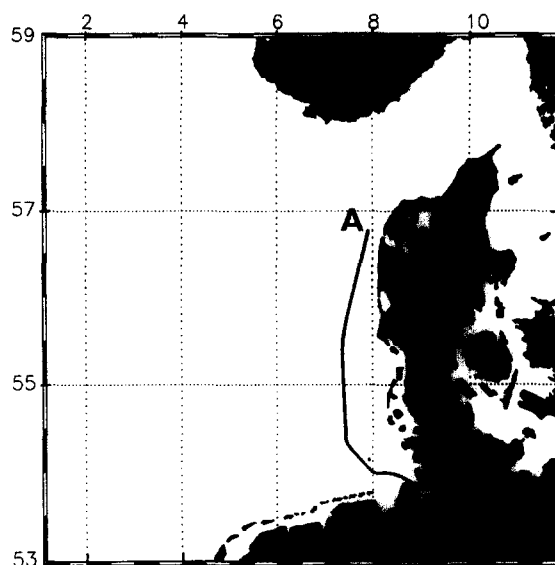

Fig. 4. Location of transect A–B during R/V Valdivia cruise no. 148-2 in September 11–14, 1994.

the compass platform of R/V Valdivia and the airflow split for the two systems.

A consistent set of calibration gases with known amounts of CO_2 (± 0.3 ppmv) in "natural" air was used although different pressure requirements of the systems prohibited the use of the same cylinders. Nitrogen was used as a zero reference gas. The IFM system was calibrated on an hourly basis, the IOW system once during the experiment. During the 1-h calibration intervals (IFM) the NDIR analyzer remained remarkably stable with a drift in the order of $+0.1$ μmol/mol. The 24-h interval was correspondingly accompanied by a drift of the CO_2 analyzer of approx. $+2.5$ μmol/mol. The drift was not accompanied by an apparent drift of the IR cell temperature. This drift was removed linearly from the IOW data set. It was concluded that a calibration interval of 4–6 h would be a reasonable compromise.

The conversion of detector mV readings into CO_2 mole fractions based on internal algorithms (1) to (5) of the LI-COR analyzer and the calculation of partial pressure of CO_2 according to Eqs. (6) and (7) was performed identically for the to data sets comprising the following steps:

1. user calibration of the IR analyzer by setting the "zero point" as an offset z (calculated from measurement of a CO_2-free calibration gas) and

"span" as a factor s (calculated from measurement of a calibration gas with known CO_2 mixing ratio), applied internally to the raw detector readings mV:

$$mV^* = s \cdot mV + z$$

2. the mV^* readings are linearly corrected from the cell pressure p (kPa) during the measurement to a pressure of 1 atmosphere ($p_0 = 101.325$ kPa):

$$mV' = mV^* \cdot \frac{p_0}{p}$$

3. the CO_2 mole fraction xCO_2^{ws} ($\mu mol/mol$) from wet sample measurement with water vapor mole fraction xH_2O (mmol/mol) is calculated on the basis of the individual factory calibration polynomial and the pressure broadening effect of water vapor (for details see: McDermitt et al., 1993):

$$xCO_2^{ws} = \chi(xH_2O) \cdot \left(a_1 \cdot y + a_2 \cdot y^2 + a_3 \cdot y^3 + a_4 \cdot y^4 + a_5 \cdot y^5\right)$$

with

$$\chi(xH_2O) = 1 + (a_w - 1) \cdot \frac{xH_2O}{1000}$$

and

$$a_w = 1.57$$

and

$$y = \frac{mV'}{\chi(xH_2O)}$$

The "foreign gas broadening coefficient" a_w reflects the pressure broadening effectiveness of water vapor on the CO_2 measurement relative to nitrogen ($a_{N_2} = 1$). Its value has been determined experimentally (McDermitt et al., 1993). The mole fraction of water vapor xH_2O is provided by the simultaneous measurements in the H_2O channel;

4. the CO_2 mole fraction xCO_2^{ws} is linearly corrected for the deviation of cell temperature T (K) during measurement from factory calibration temperature T_0 (K):

$$xCO_2^{*,ws} = xCO_2^{ws} \cdot \frac{T}{T_0}$$

5. CO_2 mole fraction $xCO_2^{*,ws}$ is corrected (to dry air) for dilution of the gas phase by measured water vapor mole fraction xH_2O (mmol/mol).

$$xCO_2^{*,dry} = xCO_2^{*,ws} \cdot \left(\frac{1}{1 - \frac{xH_2O}{1000}}\right)$$
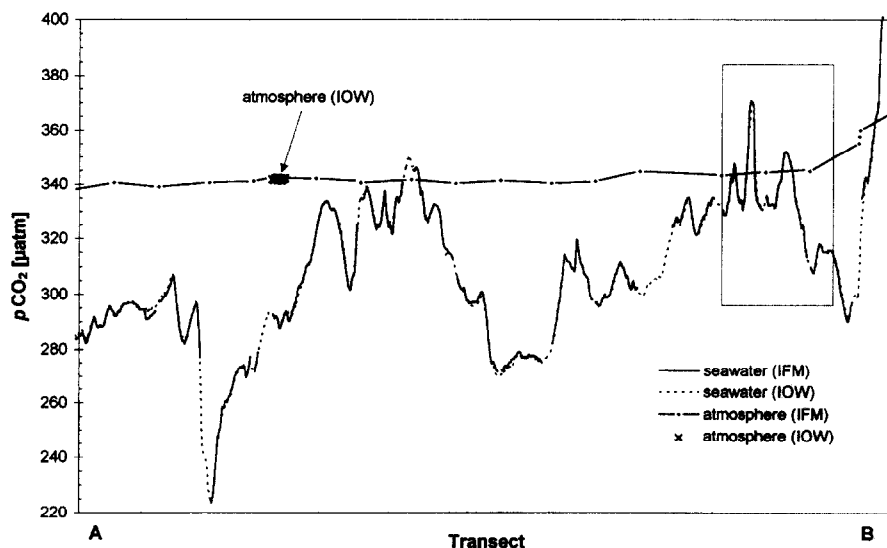

Fig. 5. Time-synchronized superposition of profiles of surface seawater and atmospheric pCO_2 on transect A–B as measured simultaneously by the IFM and IOW underway pCO_2 systems. The box indicates the location of the enlargement area in Fig. 7.

6. the pCO_2^* (μatm) at 100% humidity is calculated based on the ambient (= equilibrator) pressure p (atm) and saturation water vapor pressure w (atm).

$$pCO_2^* = xCO_2^{*,\text{dry}} \cdot (p - w)$$

The saturation water vapor pressure w (mbar) is calculated from the following equation:

$$w = 0.981 \cdot \exp\left(27.029 - 0.0098 \cdot T_{\text{abs}} - \frac{6163}{T_{\text{abs}}}\right)$$

where T_{abs} is the absolute temperature of the seawater. The seawater pCO_2 is calculated from the seawater temperature in the equilibrator while for the atmospheric pCO_2 the mixed layer temperature has to be used. If the temperature of the skin layer is known and differs from the mixed layer temperature the former should be used (Robertson and Watson, 1992). The present calculations are based on mixed layer temperatures;

7. the pCO_2^* is corrected for the temperature shift between in-situ temperature T_{is} and equilibrator temperature T_{eq} using an empirical equation

(DOE, 1994) which was originally proposed by Takahashi et al. (1993):

$$pCO_2 = pCO_2^* \cdot \exp\left(0.0423(T_{\text{is}} - T_{\text{eq}})\right)$$

4. Results and discussion

The pCO_2 profiles generated by each of two systems during the 21-h experiment were compared based on the UTC time of the 1-min intervals. A time synchronized superposition of the profiles along transect A-B (for location refer to Fig. 4) is shown in Fig. 5. The solid line (IFM) is interrupted during the hourly calibration and measurement of atmospheric pCO_2 routine while the dashed line (IOW) gives a more or less continuous record. The pCO_2 values along transect A-B are plotted against time rather than geographical position in order to display the 1-min averages equidistantly. Otherwise they would have been stretched or distorted according to the changing speed of the vessel. In any other application plotting against a distance axis instead of a
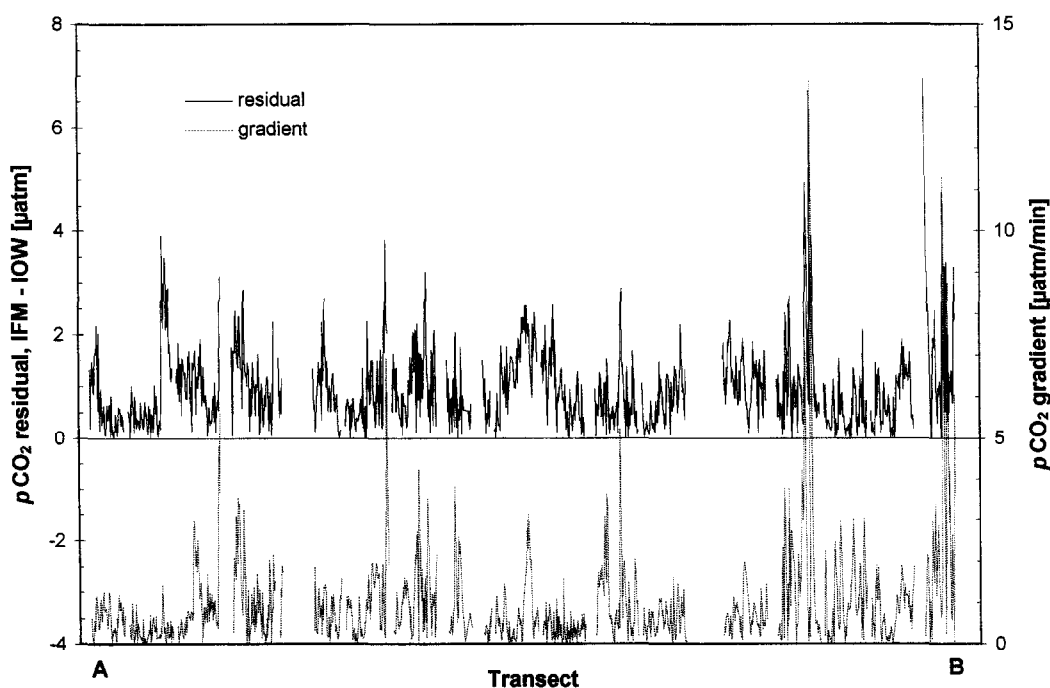

Fig. 6. Residuals of the 1-min averages of the two surface seawater pCO_2 profiles (top) and absolute values of the measured pCO_2 gradient as calculated from the IFM profile (bottom).

time axis would have been more useful but in this discussion we focus on a time synchronized comparison of the data points.

The striking feature of Fig. 5 is a marked qualitative and quantitative conformity of the profiles. Even though the North Sea offered a kind of worst case situation with a highly variable spatial pCO_2 distribution there is no significant difference in the profiles at this level. The 1-min averages of the whole experiment show a mean difference (IFM − IOW) of +0.15 μatm (IFM: 310.32 ± 29.59 μatm; IOW: 310.16 ± 29.79 μatm) which indicates that there is no systematic difference between the systems. The standard deviation of 1.2 μatm of the differences between the 1-min averages can in part be attributed to the differences occurring during high pCO_2 gradients. In most cases peaks in the differences coincide with peaks in the gradient (Fig. 6). The pCO_2 gradient as calculated from the IFM profile reached peak values as high as 10–14 μatm/min, which were followed by both systems. At a mean ship speed of appr. 8 knots a 1-min average corresponds to a distance of 250 m in which changes in the pCO_2 of up to 14 μatm were measured.

The atmospheric pCO_2 shows a steady level of approx. 342 μatm. Towards the inner German Bight the atmospheric pCO_2 level is raised by some 30

μatm which can be attributed to the influence of air masses contaminated by industrial areas of northern Germany. The single atmospheric measurement cycle carried out by the IOW system during the experiment is in full agreement with the atmospheric pCO_2 profile of the IFM system during that period (IFM: 342.24 ± 0.11 μatm; IOW: 341.84 ± 0.35 μatm).

Encouraged by the general agreement of these measurements we took a closer look at the "fine structure" of the profiles. For this purpose a 165-min interval was enlarged to reveal any further features (Fig. 7). The mean difference (IFM − IOW) of the 1-min averages in this enlargement interval is +0.5 μatm. Still the conformity of the profiles at this level is remarkable. The IFM system shows slightly higher maxima and lower minima than the IOW system with the slopes of the pCO_2 peaks being little steeper in the IFM profile (i.e., more positive in the uprise and more negative in the fall). This feature of the profiles can also be seen if the pCO_2 gradient as calculated from the IOW profile is plotted versus the pCO_2 gradient as derived from the IFM profile (Fig. 8). In a correlation analysis after Bartlett (1949) a straight line was fitted to these two variables which are subject to the same order of error. The estimated slope of 0.86 indicates that the IOW gradient is on the average by 14% lower than the IFM profile.
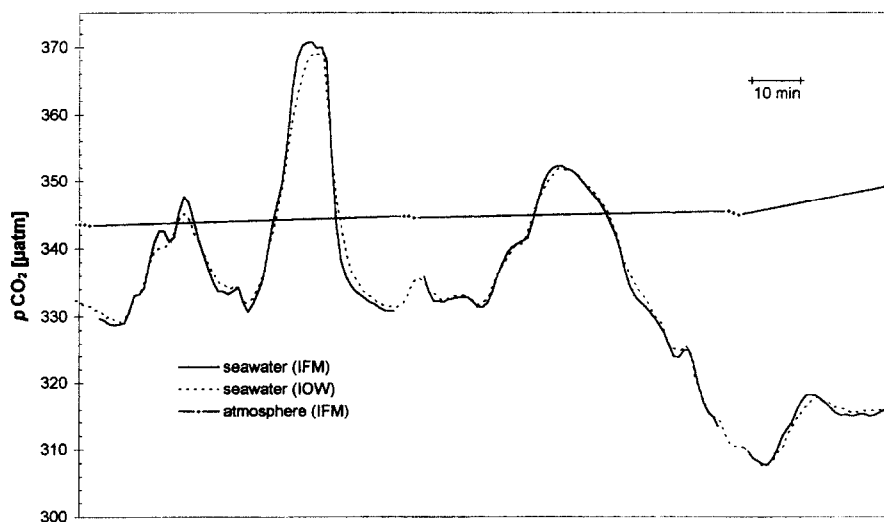

Fig. 7. Enlargement of a 165-min interval of the superimposed pCO_2 profiles. For location of the enlarged profile in the 21-h section refer to Fig. 5.

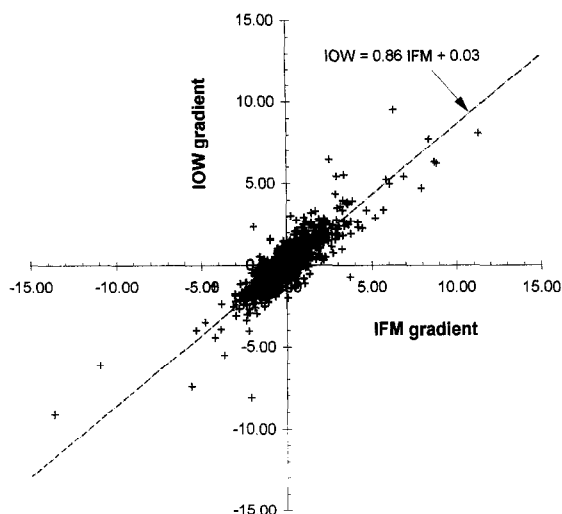Fig. 8. Plot of the $p\mathrm{CO}_2$ gradient as calculated from the IOW profile versus the $p\mathrm{CO}_2$ gradient derived from the IFM profile. The straight line was fitted to the data after a correlation analysis after Bartlett (1949).

From these findings and the qualitative examination of the profiles in Fig. 7 a slightly different time constant can be inferred.

In order to estimate the time constants a step experiment was carried out with both $p\mathrm{CO}_2$ sys-

tems. For this purpose two batches of water characterized by different $p\mathrm{CO}_2$ and T were provided in plastic bags which allowed the water to be kept out of contact with a headspace throughout the whole experiment. Both batches were run subsequently through the systems. After a steady reading of the first batch was achieved the water supply was switched steplike to the second batch and the change of measured $p\mathrm{CO}_2$ and T were followed in short time intervals (Fig. 9). Under the assumption that the re-equilibration can be described as a first-order process the following equation holds:

$$\frac{\mathrm{d}p_a}{\mathrm{d}t} = k(p_w - p_a)$$

in which p_a stands for the measured $p\mathrm{CO}_2$ in the carrier gas stream, p_w for the $p\mathrm{CO}_2$ of the water phase and k represents the rate constant of the process. Integration yields an exponential equation:

$$p_a = p_w + (p_a^0 - p_w) \cdot e^{-kt}$$

with p_a^0 and p_w being the $p\mathrm{CO}_2$ values of the first and second batch, respectively, and p_a the measured $p\mathrm{CO}_2$ at time t. A plot of $-\ln(p_a - p_w/p_a^0 - p_w)$ vs. t shows an almost perfect linear correlation thus justifying the a priori assumption of a first-order rate
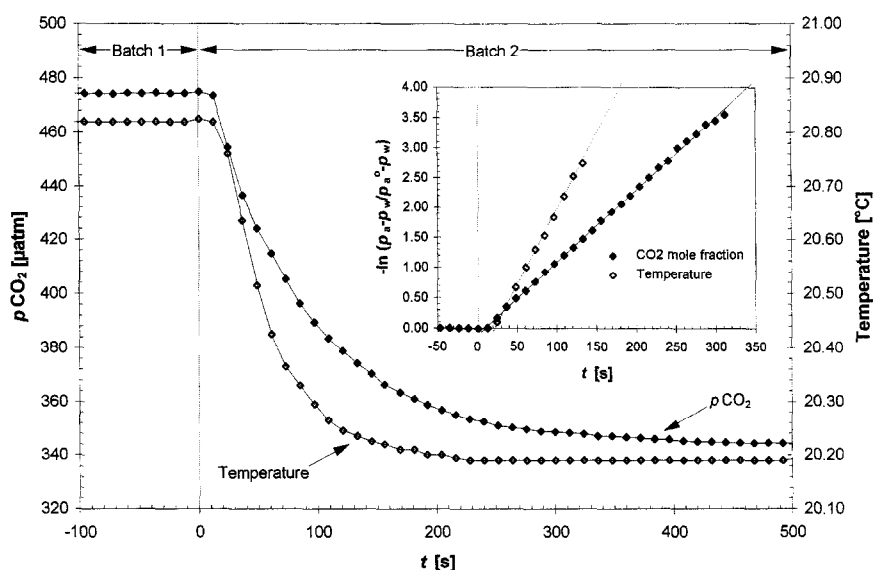

Fig. 9. Results from a step experiment with 12-s averages for $p\mathrm{CO}_2$ and water temperature (IFM system). The step from batch 1 to batch 2 occurs at $t = 0$. The insert shows a plot of $-\ln(p_a - p_w/p_a^0 - p_w)$ vs. time axis of the experiment (analogous for temperature). From the slope of the regression lines the time constants were calculated.

law (Fig. 9). The time constant $(1/k)$ can be calculated from the slope. Assuming that the heat exchange between the water and the gas phase or the equilibrator walls is small, temperature changes in the equilibrator after the change between the batches give information about the water exchange rate in the equilibrator. From experimental runs with different step directions, step magnitudes and water flow rates the following time constants for pCO_2 were evaluated: IFM system, 75 ± 6 s (42 s); IOW system, 46 ± 1 s (22 s). The numbers in parentheses give the corresponding time constants for temperature. While the time constants for pCO_2 can be regarded as overall time constants the time constants for temperature represent the physical mixing in the equilibration cell.

The results underline the observation that both systems are characterized by a fast response to pCO_2 changes. However, the slight differences between the profiles discussed above cannot be explained by the experimental time constants. One reason for this discrepancy could be the fact that seawater flow rates of the IOW system were not monitored at sea. As changing flow rates affect the time constants these may have been different at sea from the experimentally measured time constants. It should also be mentioned that as the experiment was not designed for such detailed examination the interpretability of such miniature differences is clearly limited. For example the 1-min averages were not taken fully synchronized throughout the experiment, so that they are out of phase at between 0 and 30 s. We would like to emphasize that the observed differences in the "fine structure" of the profiles are negligible with respect to the scales of the ΔpCO_2 concept.

5. Conclusions

The findings reported in this paper clearly demonstrate that an excellent at-sea agreement of data from different pCO_2 systems can be achieved. Both new systems have shown their capability of a fast response to pCO_2 changes. However, the sharing of facilities like the water supply system, in-situ temperature and pressure data and calibration gases and the identical mathematical treatment of the data have excluded possible sources of errors. As temperature and pressure measurements can be done with the necessary accuracy rather conveniently and as calibration gases can be prepared carefully enough the possible errors contributed by this can be minimized. The conclusions of this experiment are certainly somewhat restricted by the fact that two system of rather similar design were compared. The results may therefore be regarded as a first check at-sea under ideal circumstances. Encouraged by the reported excellent agreement a next step should be a more general at sea intercomparison of underway pCO_2 systems which includes systems of very different design.

References

Bartlett, M.S., 1949. Fitting a straight line when both variables are subject to error. Biometrics, 5: 207–212.

Copin-Montegut, C., 1985. A method for the continuous determination of the partial pressure of carbon dioxide in the upper ocean. Mar. Chem. 17: 13–21.

Copin-Montegut, C., 1988. A new formula for the effect of temperature on the partial pressure of CO_2 in seawater. Mar. Chem., 25: 29–37.

Copin-Montegut, C., 1989. A new formula for the effect of temperature on the partial pressure of CO_2 in seawater (corrigendum). Mar. Chem., 27: 143–144.

DOE, 1994. A.G. Dickson and C. Goyet (Editors), Handbook of Methods for the Analysis of the Various Parameters of the Carbon Dioxide System in Sea Water, Version 2. ORNL/CDIAC-74.

Gordon, L.I. and Jones, L.B., 1973. The effect of temperature on carbon dioxide partial pressure in seawater. Mar. Chem., 1: 317–322.

Goyet, C. and Peltzer, E., 1994. Comparison of the August–Sep-

tember 1991 and 1979 surface partial pressure of CO_2 distribution in the Equatorial Pacific Ocean near 150°W. Mar. Chem., 45: 257–266.

Goyet, C., Beauverger, C., Brunet, C. and Poisson, A., 1991. Distribution of carbon dioxide partial pressure in surface waters of the Southwest Indian Ocean. Tellus, 43B: 1–11.

Goyet, C., Millero, F.J., Poisson, A. and Shafer, D.K., 1993. Temperature dependence of CO_2 fugacity in seawater. Mar. Chem., 44: 205–219.

Houghton, J.T., Jenkins, G.T. and Ephraums, J.J., 1990. Climate Change — The IPCC Scientific Assessment. Cambridge Univ. Press, Cambridge.

Inoue, H., Sugimura, Y. and Fushimi, K., 1987. pCO_2 and $\delta^{13}C$ in the air and surface sea water in the western North Pacific. Tellus, 39B: 228–242.

Keeling, C.D., Rakestraw, N.W. and Waterman., L.S., 1965. Carbon dioxide in surface waters of the Pacific ocean. 1. Measurements of the distribution. J. Geophys. Res., 70: 6087–6097.

Keeling, C.D., Whorf, T.P., Wahlen, M. and van der Plicht, J., 1995. Interannual extremes in the rate of rise of atmospheric carbon dioxide since 1980. Nature, 375: 666–670.

Kelley Jr., J.J., 1970. Carbon dioxide in the surface waters of the North Atlantic Ocean and the Barents and Kara Seas. Limnol. Oceanogr., 15: 80–97.

Kimoto, T. and Harashima, A., 1993. High resolution time/space monitoring of the surface seawater CO_2 partial pressure by ship-of-opportunity. Paper presented at the 4th Int. CO_2 Conf., Carqueiranne, September 14–19.

Liss, P.S., 1983. Gas transfer: experiments and geochemical implications. In: P.S. Liss and W.G.N. Slinn (Editors), Air–Sea Exchange of Gases and Particles. Reidel, Dordrecht, pp. 241–298.

Liss, P.S. and Merlivat, L., 1986. Air–sea exchange rates: introduction and synthesis. In: P. Buat-M-nard (Editor), The Role of Air–Sea Exchange in Geochemical Cycling. Reidel, Dordrecht, pp. 113–127.

McDermitt, D.K., Welles, J.M. and Eckles, R.D., 1993. Effects of temperature, pressure and water vapor on gas phase infrared absorption by CO_2. Poster and manuscript presented at the AGU Fall Meeting, San Francisco, December 6–10.

Ohtaki, E., Yamashita, E. and Fujiwara, F., 1993. Carbon dioxide in surface sea waters of the Seto Inland Sea. Jpn. J. Oceanogr., 49: 295–303.

Poisson, A., Metzl, N., Brunet, C., Schauer, B., Bres, B., Ruiz-Pino, D. and Louanchi, F., 1993. Variability of sources and sinks of CO_2 in the Western Indian and Southern Oceans during the year 1991. J. Geophys. Res., 98(C12): 22,759–22,722, 22,778.

Robertson, J.E. and Watson, A.J., 1992. Thermal skin effect of the surface ocean and its implications for CO_2 uptake. Nature, 358: 738–740.

Robertson, J.E., Watson, A.J., Langdon, C., Ling, R.D. and Wood, J.W., 1993. Diurnal variations in surface pCO_2 and O_2 at 60°N, 20°W in the North Atlantic. Deep-Sea Res., 40: 409–422.

Schneider, B., Kremling, K. and Duinker, J.C., 1992. CO_2 partial pressure in Northeast Atlantic and adjacent shelf waters: Processes and seasonal variability. J. Mar. Syst., 3: 453–463.

Takahashi, T., 1961. Carbon dioxide in the atmosphere and in Atlantic Ocean water. J. Geophys. Res., 66: 477–494.

Takahashi, T., Olafsson, J., Goddard, J.G., Chipman, D.W. and Sutherland, S.C., 1993. Seasonal variation of CO_2 and nutrient salts in the high latitude oceans: a comparative study. Global Biogeochem. Cycles, 7: 843–848.

Tans, P.P., Fung, I.Y. and Takahashi, T., 1990. Observational constraints on the global atmospheric CO_2 budget. Science, 247: 1431–1438.

Wallace, D.W.R., 1995. Monitoring global ocean carbon inventories. Ocean Observing System Development Panal, Texas A&M Univ., College Station, TX, 54 pp.

Wanninkhof, R., 1992. Relationship between wind speed and gas exchange over the ocean. J. Geophys. Res., 97: 7373–7382.

Watson, A.J., Nightingale, P.D. and Cooper, D.J., 1995. Modelling atmosphere–ocean CO_2 transfer. Philos. Trans. R. Soc. London B, 348: 125–132.

Weiss, R.F., 1974. Carbon dioxide in water and seawater: the solubility of a non-ideal gas. Mar. Chem., 2: 203–215.

Weiss, R.F., 1981. Determinations of CO_2 and methane by dual catalyst flame ionization chromatography and nitrous oxide by electron capture chromatography. J. Chromatogr. Sci., 19: 611–616.

Weiss, R.F., Jahnke, R.A. and Keeling, C.D., 1982. Seasonal effects of temperature and salinity on the partial pressure of CO_2 in seawater. Nature, 300: 511–513.